Effect of Fullerene C_{60} on the Melt Grafting Reaction between Multifunctional Monomer and Polypropylene

Dong Wan,[1,2] Haiping Xing,[1,2] Zhenjiang Zhang,[1,2] Yujie Wang,[1,2] Lu Wang,[1,2] Yanhui Wang,[1] Zhiwei Jiang,[1,2] Tao Tang[1]

[1]State Key Laboratory of Polymer Physics and Chemistry, Changchun Institute of Applied Chemistry, Chinese Academy of Sciences, Changchun 130022, People's Republic of China
[2]Graduate School of the Chinese Academy of Sciences, Beijing 100039, China
Correspondence to: T. Tang (E-mail: ttang@ciac.jl.cn)

ABSTRACT: Effect of different content of C_{60} on the melt radical reaction between trimethylol propane triacrylate (TMPTA) and polypropylene (PP) was studied by means of Fourier transform infrared, melt torque values, and rheological results. C_{60} could transfer most of the reactive PP macroradicals to more stable macroradicals at first due to its higher reaction rate with radicals. Therefore, the homopolymerization of TMPTA was restrained to some extent. PP samples containing TMPTA, C_{60}, and 2,5-dimethyl-2,5(*tert*-butylperoxy) hexane peroxide (DHBP) showed a more obvious influence on increasing the entanglements between PP chains comparing with PP samples containing C_{60} and DHBP, owing to the synergetic effect between TMPTA and C_{60} on branching with PP macroradicals. © 2012 Wiley Periodicals, Inc. J. Appl. Polym. Sci. 000: 000–000, 2012

INTRODUCTION

Polypropylene (PP) is one of the most widely produced and used plastics due to its higher melting temperature, low density, chemical resistance, and better mechanical properties. However, commercial isotactic PP, mainly prepared by Ziegler–Natta catalysts, cannot be applied into some processes, where elongational properties and melt strength are dominant, such as foaming, blowing, and extrusion coating, mainly because of the linear structure. Fractions of long chain branched or crosslinked structure in PP has been verified to be an effective way to confer PP with obvious strain hardening in extensional flows and enhance melt strength as a result of the increase of the entanglements between polymer chains.[1–3]

Melt mixing is a more convenient and economic approach to prepare high melt strength PP (HMSPP), comparing with *in situ* polymerization in a reactor[4,5] and high-energy irradiation[6,7] due to the absence of solvent and short processing time. Several methods have been used to enhance the melt strength of PP via melt mixing according to the previous reports: chemical reactions between the grafted groups on PP, such as epoxy and maleic anhydride,[8] amine and maleic anhydride,[9] and amine and glycidyl;[10] blending linear PP with branched PP[11,12] or other polymers, like Polyamide 66;[13] radical combination between PP macroradi-

cals[14,15] or radical addition between PP macroradical and multifunctional monomer (mainly containing reactive C=C bonds).[16–20] Recently, the method of radical addition was mostly used to prepare HMSPP. However, β-scission of PP macroradicals and homopolymerization of multifunctional monomers in the presence of high content of free radicals are the main side reactions.[16–19] The former reaction will lead to the chain scission and reduce the melt strength of PP. The latter reaction will result in the lower branching efficiency of multifunctional monomers. Thiuram disulfide[16] and dithiocarbamate[17,18] were found to effectively promote the branching reaction between PP macroradicals and trimethylol propane triacrylate (TMPTA) and limit the β-scission by decreasing the instantaneous concentration of free radicals through reversible radical reaction at high temperature. Heteroaromatic ring derivatives,[19,21,22] with the heteroaromatic ring conjugated with a double bond bearing electron-attracting groups substituent, display a high addition rate to the macroradical with the formation of resonance stabilized radicals, thus can decrease the content of high reactive PP macroradicals. In our previous research,[19] we found different heteroaromatic ring derivatives, especially 1-cyano-3-(furan-2-yl)-2-propenoic acid ethyl ester (CFA) and 2-(furan-2-ylmethylene)malononitrile (FN), could obviously promote the branching efficiency of TMPTA and increase the chain entanglements between polymer chains.

As a special nanoparticle of single molecule, fullerene C_{60} has a high electron affinity (ca. 2.7–2.8 eV) and is therefore capable of acting as radical scavengers. C_{60} has 30 carbon–carbon double bonds, which can trap more than 34 free radicals; thus, it is known as a radical sponge.[23] In our previous researches,[24,25] we have demonstrated that the interfacial reaction between C_{60} and PP took place in the presence of peroxide by simple melt mixing. Not only the dispersion state of C_{60} nanoparticles was improved but also the chain structure of PP changed a lot in the presence of peroxide. The reaction between methyl radical and C_{60} was very fast with the rate constant about 4.6×10^8 M^{-1} S^{-1}.[26] However, the rate constant between methyl radical and methyl methacrylate was about 10^5–10^6 M^{-1} S^{-1}.[27] So, in principle, C_{60} can react with PP macroradicals at first and reduce the concentration of reactive PP macroradicals, and finally, homopolymerization of TMPTA can be restrained.

In this work, we studied the influence of the content of C_{60} on the melt grafting reaction between PP macroradicals and TMPTA molecules. The possible reactions and microstructures of the modified PP samples were proposed according to our experimental results.

EXPERIMENT

Materials
Additive-free isotactic PP powder (melt flow rate (MFR) = 2.0 g/10 min) was supplied by Daqing Petrochemical Corporation, China. C_{60} (purity: 99.9%) was purchased from Yongxin Technology, Henan province, China 2, 5-dimethyl-2, 5(*tert*-butyl-peroxy) hexane peroxide (DHBP) was obtained from Aldrich. TMPTA was obtained from Tianjin Tianjiao Chemical, China. Other reagents were used without further purification.

Sample Preparation
All samples were prepared via melt mixing at 180°C for 8 min using a Brabender LH60 internal mixer (Shanghai, China) with a rotating speed of 64 rpm. The detailed composition of different modified PP samples was listed in Table I. Torque curves were acquired by Brabender mixing software. Before melt mixing, about 45 g PP power with a designed composition of C_{60}, TMPTA, and DHBP was premixed by high speed pulverator for 2 min. Sample PP was mixed with 0.2 wt % Irganox B215 at the beginning of melt mixing, and other samples were mixed with 0.2 wt % B215 after melt mixing about 7 min. After melt mixing, the samples were shaped into 1 mm thick by compressing molding at 180°C. The resultant samples were designated as xTyCzD. Herein, T, C, and D denote TMPTA, C_{60}, and DHBP, respectively; and $x, y,$ and z denote the weight percentage of TMPTA ($\times 10$), C_{60} ($\times 10$), and DHBP ($\times 100$), respectively. For example, 12T12C010D means that the sample contains 1.2 wt % TMPTA, 1.2 wt % C_{60}, and 0.1 wt % DHBP.

Characterization
Fourier Transform Infrared (FTIR) (Bio-RadFTS-135) was used to characterize plain PP and modified PP samples. Before measurements, the modified samples were dissolved in xylene for 2 h at 140°C with 0.2 wt % 2,6-di-*tert*-butyle-4-methylphenol (BHT). The extracted solution was charged into acetone at room temperature. The precipitates were filtrated and extracted

Table I. The Detailed Composition of Different Modified PP Samples

Sample	TMPTA (wt %)	C_{60} (wt %)	DHBP (wt %)
PP	0	0	0
12C	0	1.2	0
010D	0	0	0.1
01C010D	0	0.1	0.1
05C010D	0	0.5	0.1
12C010D	0	1.2	0.1
12T	1.2	0	0
12T010D	1.2	0	0.1
12T01C010D	1.2	0.1	0.1
12T05C010D	1.2	0.5	0.1
12T12C010D	1.2	1.2	0.1

with boiling acetone for 12 h to remove the residual multifunctional monomer. The precipitates were dried at 70°C for at least 24 h under vacuum, and then pressed into thin films at 180°C for FTIR measurements.

For measuring the content of gel, about 0.5 g modified PP sample was cut into small pieces and then packed with nylon fabric of 500 meshes. The weights of PP and nylon fabric were recorded as w_0 and w_1, respectively. The packed PP sample was extracted in boiling xylene for 12 h. After extraction, the nylon package was dried at 80°C for at least 36 h, and then, the weight was recorded as w_2. The gel content was determined by the formula:

$$\text{Gel} = \frac{w_2 - w_1}{w_0} \times 100\% \qquad (1)$$

The rheological properties were measured on PHYSICA MCR 300 (Anton Paar GmbH, Austria) under nitrogen atmosphere. Round samples (25 mm in diameter $\times$ 1 mm in thickness) were prepared for frequency scanning at 180°C, with a gap of 0.8 mm and a frequency scope from 0.01 to 100 rad s^{-1}. The strain was fixed at 1% to make the materials be in the linear viscoelastic region.

The extensional experiments were performed at 180°C using the extensional viscosity fixture on ARES-G2 from TA instruments, America with different Hencky extension rates: 0.05, 0.1, 0.5, and 1 s^{-1}. Photographs were taken per second to observe the intermediate state of the sample.

RESULTS AND DISCUSSION

At first, model experiments were done to investigate the influence of C_{60} on the homopolymerization of TMPTA at 180°C. TMPTA alone polymerized to form a piece of solid crosslinked polymer at 4 min. However, TMPTA containing 0.1 and 1.0 wt % C_{60} polymerized at 6.5 and 16 min under the same conditions, respectively. From the above results, we can conclude that the reactivity of C_{60} toward free radicals is much higher than that of TMPTA. On one hand, C_{60} can quickly transfer the high reactive radicals to more stable radicals; on the other hand, the
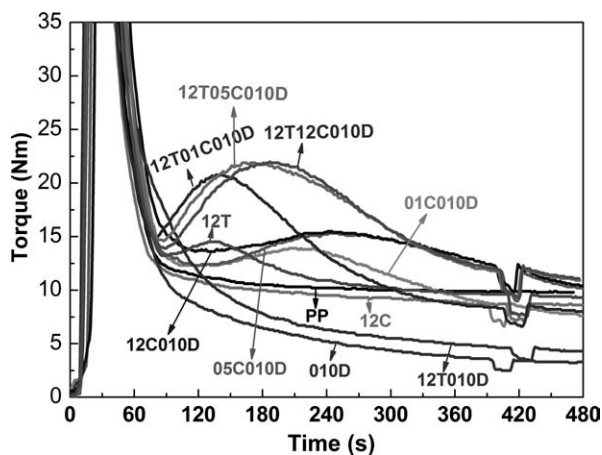
**Figure 1.** Behavior of the mixing torque for plain PP and modified PP samples.

stable radicals can not react with the C=C bond in TMPTA monomer or the reaction proceeds very slowly.

Both C_{60} and TMPTA can react with more than two PP macroradicals; however, their mixing torque curves show much differences. It is well accepted that the torque value is proportional to the melt viscosity of the polymer,[28] and the chain extension reactions can increase the mixing torque.[18,21] As shown in Figure 1, without DHBP, Sample 12C showed a slight decrease

of torque values comparing with PP due to the minor degradation of PP matrix.[24] However, Sample 12T had a new torque peak after complete fusion of PP. It was because that PP macroradicals generated from thermal degradation attacked the C=C bond in the TMPTA and the homopolymerization of TMPTA [Scheme 1, Reactions (2b), (2c), and (2d)]. In the presence of DHBP, PP samples containing C_{60} showed a different changing trend comparing with those containing TMPTA. Several PP macroradicals attacked the C=C bonds on the surface of one C_{60} molecule or one C_{60} cluster that led to form long chain branched structure;[24] therefore, a new torque peak of the Samples 01C010D, 05C010D, and 12C010D appeared. However, comparing with 12T, the TMPTA molecules in Sample 12T010D were consumed quickly due to the severe homopolymerization at a high concentration of free radicals [Scheme 1, Reactions (3b) and (3f)]. Consequently, the torque values decreased with the mixing time after complete fusion of PP due to the degradation of PP chains. However, the torque values of PP samples containing C_{60} and TMPTA simultaneously increased obviously from 90 to 300 s.

For better description of the torque curves, we defined several variables. As shown in Figure 2, t_0 represents the time that the melt viscosity starts to increase after complete fusion of PP, and Δt represents the time span between t_0 and the time of the maximum torque value. T_{max} and T_{end} represents the maximum torque value and the end torque value after complete fusion of
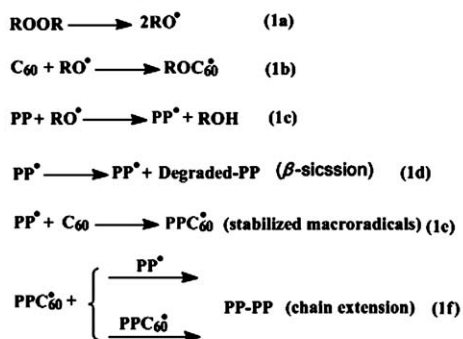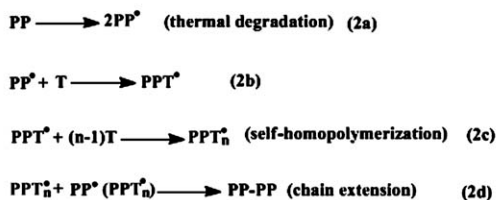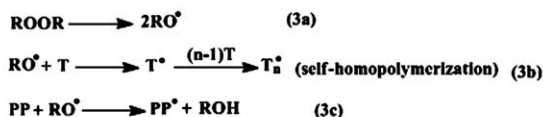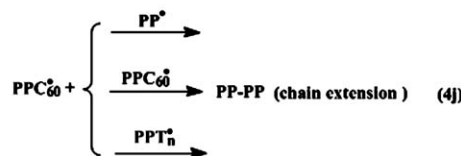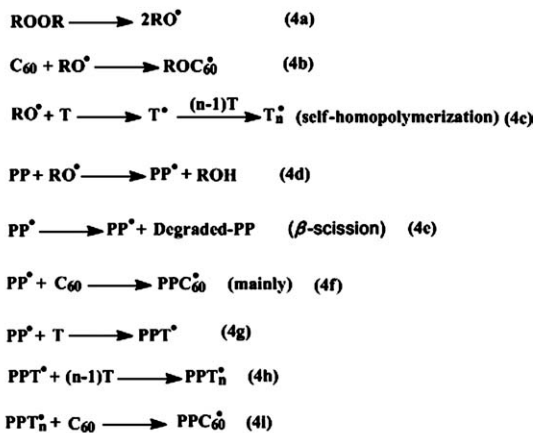

Scheme 1. Possible reactions involved during melt radical grafting process.
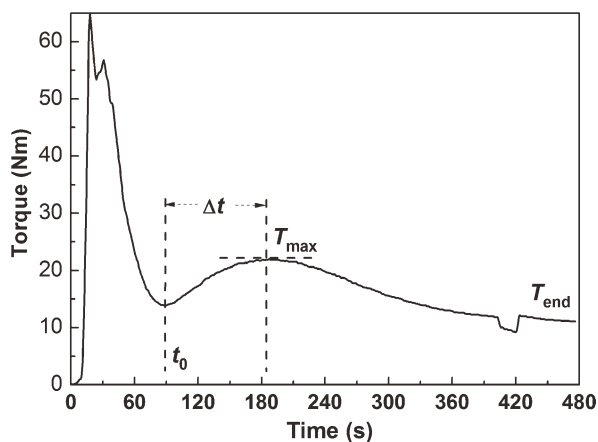
Figure 2. Schematic showing the definition of several variables of torque curve.

PP. Before t_0, the melt or degradation of PP chains predominated on the melt viscosity. However, during Δt, the influence of chain extension reaction on the melt viscosity was stronger than that of chain scission on the melt viscosity. The corresponding results were summarized in Table II. For PP samples containing C_{60} and DHBP, the t_0 decreased but Δt increased with the increasing content of C_{60}. C_{60} is very reactive toward free radicals, especially carbon-centered radicals.[29] Therefore, it can quickly combine with PP macroradicals and transfer the high reactive PP macroradicals to more stable macroradicals [Scheme 1, Reaction (1e)]. Comparatively, the β-scission of PP macroradicals was restrained [Scheme 1, Reaction (1d)]. The more C_{60} added, the more $PPC_{60}^{\bullet}$ was formed. From Reaction (1f) in Scheme 1, it can be concluded that the chain extension reaction was strongly influenced by the concentration of $PPC_{60}^{\bullet}$. Consequently, Sample 12C010D had a smaller t_0 and longer Δt comparing with 01C010D or 05C010D. However, both t_0 and Δt of PP samples containing TMPTA, C_{60}, and DHBP increased with the content of C_{60}. There was no torque

peak of Sample 12T010D after complete fusion of PP due to the severe homopolymerization of TMPTA at high concentration of free radicals [Scheme 1, Reactions (3b) and (3f)].[16–18] Further adding C_{60}, most of the free radicals were converted to more stable macroradicals [Scheme 1, Reactions (4b) and (4f)], and the corresponding Reaction (4g) was restrained. The more C_{60} added, the less $PPT^{\bullet}$ was formed. Though the reactivity of C=C in C_{60} is much higher than that in TMPTA toward free radicals, the viscosity increased quickly for PP samples containing TMPTA due to the easy homopolymerization of TMPTA molecules. This was verified by the mixing torque curves, PP samples containing TMPTA, C_{60}, and DHBP had much lower t_0 and Δt than PP samples containing C_{60} and DHBP. 12T12C010D had much higher concentration of $PPC_{60}^{\bullet}$ and lower concentration of $PPT^{\bullet}$ compared with 12T01C010D or 12T05C010D. Therefore, during Δt period of the Sample 12T01C010D, the torque values of PP samples containing TMPTA, C_{60}, and DHBP decreased, but t_0 increased with the increasing content of C_{60}. The T_{max} and T_{end} of 12T12C010D increased to 22.0 and 11.1 Nm, compared with these of 12C010D (only 15.5 and 10.2 Nm) owing to the increasing entanglements between polymer chains.

FTIR spectroscopy was used to investigate the possible grafting mechanism. The unreacted TMPTA monomers and homopolymerized TMPTA (without grafting onto PP chains) were removed with acetone. As shown in Figure 3, there was a new peak at 723 cm^{-1} for Samples 12C010D and 12T12C010D, which belongs to the bending vibration of the C—C bond of the structure $C_{59} \sim$C—C$\sim$R.[30] It demonstrated that C_{60} was covalently grafted onto PP chains by radical reaction. But, the peak intensity of Sample 12T12C010D was weaker than that of 12C010D, due to the consumption of some PP macroradicals by TMPTA. Figure 4 shows the FTIR spectra of the purified samples. For all the samples modified with TMPTA, there was a band at about 1745 cm^{-1} due to the stretching vibration of the carbonyl group of the ester in the TMPTA molecule, indicating that TMPTA was grafted onto PP backbone. From the FTIR spectra, the carbonyl index (CI) was defined as A_{1745}/A_{1168},

Table II. The Melt Properties and Structural Parameters of PP and Modified PP Samples

Sample	t_0 (s)	Δt (s)	T_{max} (Nm)	T_{end} (Nm)	Gel[a] (wt %)	GD of TMPTA (wt %)	Terminal slope of G'	$\eta^*_{0.01 \text{ rad s}^{-1}}$ (10^3 Pas)	$G'_{0.01 \text{ rad s}^{-1}}$ (Pa)	$G''_{0.01 \text{ rad s}^{-1}}$ (Pa)
PP	–	–	–	9.8	0	–	1.38	20.4	19.9	203
12C	–	–	–	8.6	0	–	1.40	10.5	6.27	104
010D	–	–	–	3.4	0	–	1.60	0.6	–	–
01C010D	128	99	13.9	7.6	0	–	1.03	17.0	39.8	165
05C010D	123	119	15.3	10.0	0	–	0.71	66.0	319	578
12C010D	119	122	15.5	10.2	0	–	0.72	61.9	279	552
12T	90	39	14.5	9.3	3.38	1.06	1.07	17.7	26.9	175
12T010D	–	–	–	4.3	0	0.99	1.41	1.4	–	–
12T01C010D	83	54	20.8	8.0	0	0.81	0.92	20.4	56.4	196
12T05C010D	89	72	21.9	10.9	16.32	0.74	0.54	105.0	732	759
12T12C010D	91	96	22.0	11.1	18.55	0.66	0.64	77.8	465	623

[a]The content of gel.
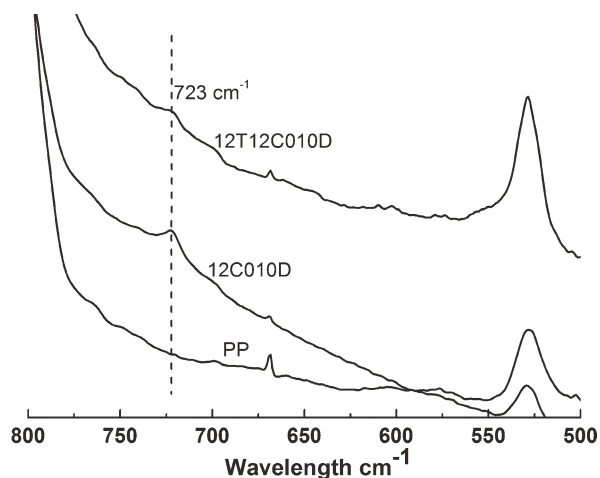
Figure 3. FTIR spectra (500–800 cm^{-1}) of various samples.

Figure 5. Calibration curve for the determination of the weight percentage of grafted TMPTA monomers.

where A_{1745} is the absorbance at 1745 cm^{-1}, characteristic of carbonyl groups of the ester; A_{1168} is the absorbance at 1168 cm^{-1}, characteristic of the CH$_3$ groups (stretching of the C—CH$_3$ groups on PP chains).[21] The CI can be considered as a measure of the content of grafted TMPTA (either in a single unit or poly chains) on the PP backbone. Because CI was a relative value, a calibration curve was constructed to achieve the grafting degree (GD). The mixtures with known amounts of TMPTA and PP were prepared by melt mixing. The calibration curve is presented in Figure 5. According to the CI values and the calibration curve, the GD of TMPTA was calculated and listed in Table II. The GD of TMPTA for Sample 12T was 1.06 wt %, suggesting that most of the TMPTA molecules was grafted onto PP backbone. However, the GD of TMPTA for PP samples containing TMPTA, C$_{60}$, and DHBP decreased with increasing the content of C$_{60}$.

The gel content of the different samples was listed in Table II. There was no gel in PP samples containing C$_{60}$ and DHBP because the content of DHBP was lower than 0.25 wt %.[24] Owing to the serious homopolymerization of TMPTA in the
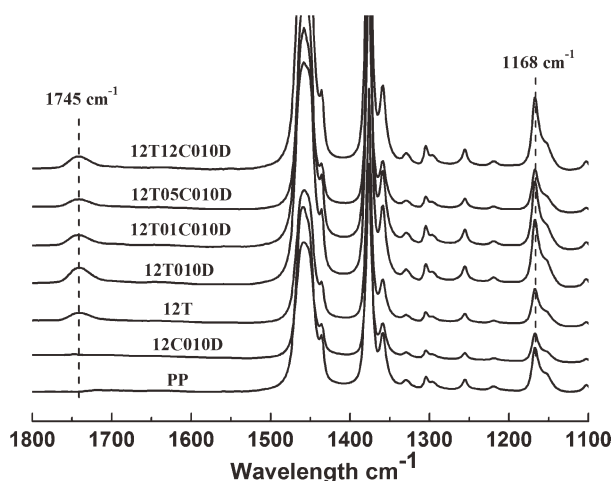
presence of peroxide, no gel was detected in 12T010D and 12T01C010D. Many domains of TMPTA homopolymers with the diameter about 100 nm were found in the PP matrix in the presence of peroxide according to our former report.[19] However, the gel content in 12T05C010D and 12T12C010D was 16.32 and 18.55, respectively.

It is well established that molecular architecture is critical to polymer melt flow behavior and processing.[31,32] Figure 6 shows the storage modulus (G') versus angular frequency (ω) for plain PP and modified PP samples at 180°C. The value of G' and the terminal slope of G' at low frequency region, reflecting the longest relaxation time, are very sensitive to the topological structure of macromolecules. The value of G' at 0.01 rad s^{-1} and the terminal slope of G' at low frequency region were summarized in Table II. Comparing with PP, 12C showed a decrease of G' at low frequency region and minor increase in the terminal slope of G' due to the thermal degradation of PP matrix at high temperature. However, 12T had larger G' at low frequency region and lower terminal slope of G' than PP due to the branching or even crosslinking reaction between TMPTA and PP macroradicals generated from thermal degradation. In the presence of
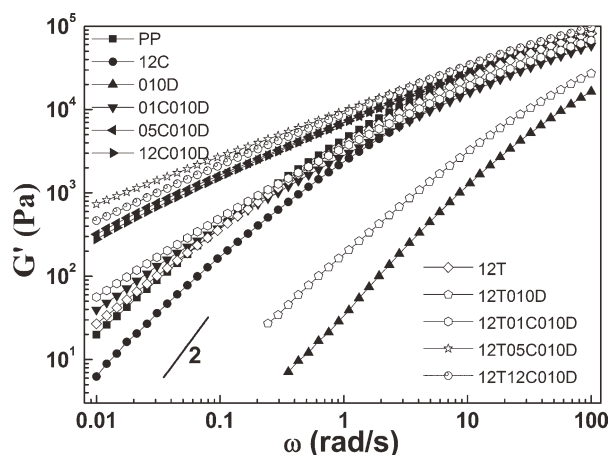

Figure 4. FTIR spectra (1100–1800 cm^{-1}) of PP and modified PP samples after purification.

Figure 6. Storage modulus versus angular frequency for plain PP and modified PP samples.
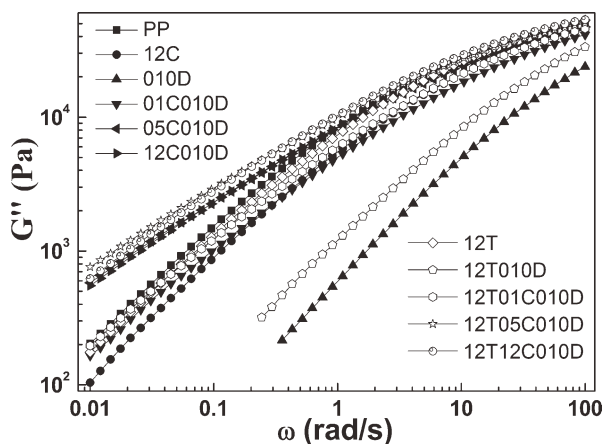
Figure 7. Loss modulus versus angular frequency for plain PP and modified PP samples.

Figure 9. Van Gurp–Palmen plots for plain PP and modified PP samples.

DHBP, 12T010D showed an obvious decrease of G' at both high and low frequency region owing to the serious homopolymerization of TMPTA molecules and dramatic degradation of PP chains at high content of free radicals. But, PP/C_{60} nanocomposites containing DHBP showed an obvious increase of G' at low frequency region, especially Samples 05C010D and 12C010D, due to the formation of long chain branched structure. For PP samples containing TMPTA, C_{60}, and DHBP, C_{60} could transfer most of high reactive PP macroradicals to more stable radicals, and therefore the homopolymerization of TMPTA was restrained. From the rheological results, the G' at 0.01 rad s^{-1} of 12T05C010D increased from 319 Pa to 732 Pa and the terminal slope of G' decreased from 0.71 to 0.54 comparing with those of 05C010D due to the synergistic effect between TMPTA and C_{60} to branch PP macroradicals and increase chain entanglements between PP chains.

Figure 7 shows the loss modulus (G'') versus angular frequency for plain PP and modified PP samples at 180°C. G'' measures the energy dissipated as heat, representing the viscous portion. The curves of G'' had almost the same changing trend with those of G'. However, G'' is not as sensitive as G' with the long
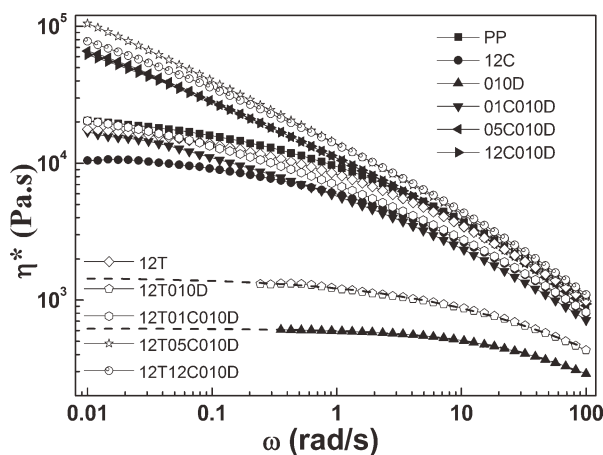
chain branched or crosslinked structure. As shown in the Table II, the G'' at 0.01 rad s^{-1} of 12T05C010D increased only from 578 to 759 Pa.

The presence of very low amounts of long chain branched structure can change complex viscosity (η^*) at low frequency region and the degree of shear thinning, when compared with the linear polymers with similar molecular weight.[33] The η^* plots of plain PP and modified PP samples are shown in Figure 8. The black dotted lines in Figure 8 were used to extend the frequency region of 010D and 12T010D according to cross-equation written as follows:[34,35]

$$\eta * (\omega) = \frac{\eta_0}{[1 + (\lambda \omega)^n]} \quad (2)$$

where η_0 is the Newtonian viscosity (also called zero-shear viscosity), λ is a relaxation time, and n is a shear-thinning index. For some of the samples, a continuous shear thinning region is observed in all frequency range, without practically any symptom of leveling off at low frequencies. In these cases, the value of the parameter η_0, which is frequency-independent can hardly be associated to the linear viscosity of the general linear

Figure 8. Complex viscosity versus angular frequency for plain PP and modified PP samples.

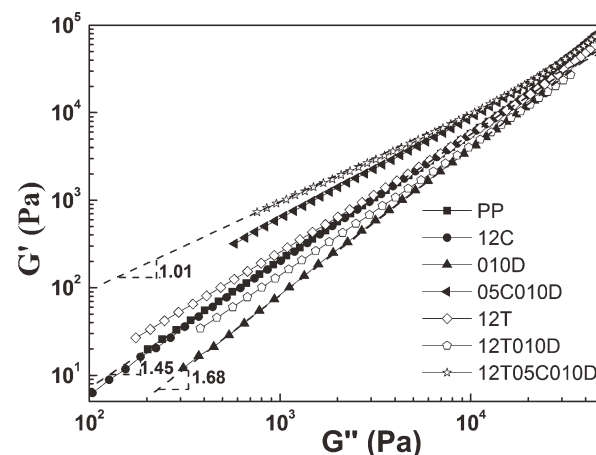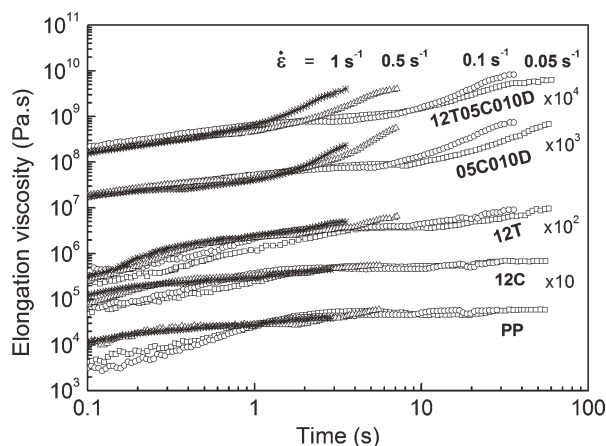**Figure 10.** Han plots for plain PP and some modified PP samples.

Figure 11. Elongational viscosity as a function of time at different Hencky strain rates.

viscoelastic model.[36] Therefore, we have approximated η_0 with the η^* measured at $\omega = 0.01$ rad s^{-1}, and the results were listed in Table II. Comparing with PP, adding DHBP alone (Sample 010D) or both DHBP and TMPTA (Sample 12T010D) led to an obvious reduction of η_0 and broader Newtonian-zone, due to the dramatic degradation of PP chains. However, the η_0 of 05C010D was about three times larger than that of PP. What is more, the η_0 of 12T05C010D increased to 105,000 Pas due to the more remarkable shear-shinning behavior.

The plot of loss angle (δ) as a function of the absolute value of complex modulus ($|G^*|$), the so-called vGP plot proposed by van Gurp and Palmen,[37] can be used to evaluate the topological structures of polymers.[38,39] Materials are almost completely viscous when the δ is close to 90° and almost completely elastic when the δ value is close to 0°. As shown in Figure 9, there was only a little difference between 01C010D and 12T01C010D. It was because that 0.1 wt % C_{60} could only consume a small amount of PP macroradicals, and most of TMPTA molecules homopolymerized to form gel-like particles in the presence of high content of radicals. However, 0.5 wt % C_{60} was enough to quickly transfer most of the high reactive PP macroradicals to more stable radicals, and therefore the homopolymerization of TMPTA molecules was largely restrained. Comparing with 05C010D or 12C010D, further adding TMPTA led the curves to become level or downturning at low $|G^*|$ due to the increasing entanglements between PP chains.[40]

The Han plot (log G' − log G'') has been proven to be a useful tool to investigate the effects of long chain branched structure on rheological properties.[41,42] Han plot is independent of the melt temperature and weight average molecular weight for monodispersed polymers. As shown in Figure 10, the Han plot of PP and 010D was almost a straight line, and the slope was 1.45 and 1.68, respectively, implying that the structures of PP and 010D were linear. However, an upshift from linear sample PP was observed for 12T, PP/C_{60}, and PP/TMPTA/C_{60} containing DHBP, especially for Sample 12T05C010D with the slope at low G'' about 1.01, indicating that a longer relaxation mechanism occurred.

Elongational behavior of polymer melts plays an important role in the processing techniques. Commercial isotactic PP is not fit for the process where extensional flows are dominant, such as foaming, blowing, and extrusion coating, due to the absence of strain hardening. The curves of elongational viscosity versus elongational time of PP and some modified PP samples at different Hencky strain rates ($\dot{\varepsilon}$) are presented in Figure 11. Strain hardening was observed as a sharp increase of elongational viscosity of PP/C_{60} and PP/TMPTA/C_{60} containing DHBP with elongational time at different $\dot{\varepsilon}$. However, there was no obvious upturn of elongational viscosity for PP and 12C, due to the linear structure of PP. Strain hardening behavior was also observed for Sample 12T; nevertheless, the elongational viscosity was only increased to a small content with elongational time. Comparing with 05C010D, the inflexion time that corresponds to the obvious upturn of elongation viscosity of 12T05C010D happens at an earlier time at the same $\dot{\varepsilon}$, which is ascribed to the increasing degree of entanglements between polymer chains. However, for Samples 010D and 12T010D, we could not perform elongational test due to the poor sag resistance. As shown in Figure 12, 010D and 12T010D could not support their own weight and had serious deformation during the test time. Traditionally, long chain branched structure can increase the entanglements between polymer chains and improve the sag resistance.[8] Adding 1.2 wt % TMPTA, 0.1 wt % DHBP, and only 0.1 wt % C_{60} (Sample 12T01C010D) could lead to formation of a small amount of long chain branched structure, and therefore, the sag did not influence the elongational tests.

From the above results, we can conclude that both TMPTA and C_{60} can react with PP macroradicals to introduce long chain branched structure. The C=C bonds in TMPTA are easy to react with each other to form gel-like particles in the presence of high content of radicals [Scheme 1, Reactions (3b) and (3f)]. Considering the reaction characteristic of TMPTA and the
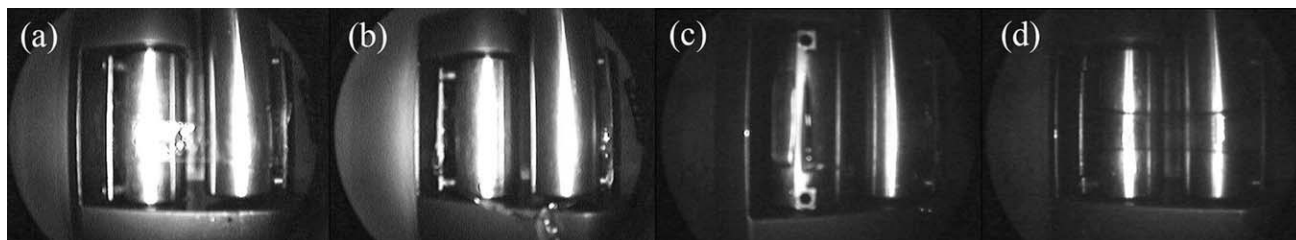

Figure 12. The photographs of plain PP and some modified PP samples during the elongational test at 180°C: (a) PP, (b) 010D, (c)12T010D, and (d)12T01C010D.
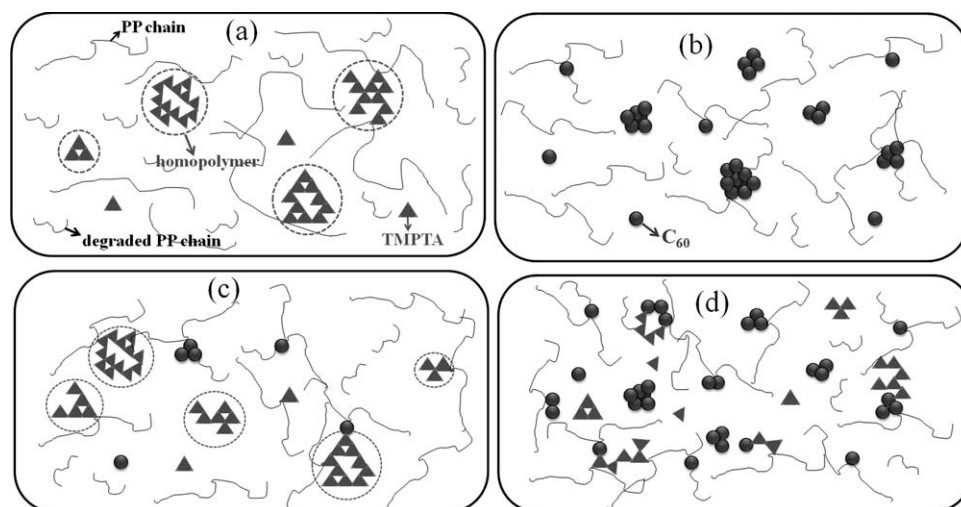
Figure 13. Schematic drawing of microstructure of different samples: (a) 12T010D, (b) 05C010D, (c) 12T01C010D, and (d)12T05C010D.

results of FTIR and rheological properties, the possible microstructure in 12T010D was proposed. As shown in Figure 13(a), some TMPTA grains with several C=C bonds on the surface reacted with PP macroradicals and few unreacted TMPTA molecules can be found in the system. This was verified by by scanning electron microscope (SEM) that some gel-like particles were found in the PP sample containing TMPTA and DHBP.[19] The G' and $\eta^\star$ of 12T010D at low frequency region decreased greatly comparing with PP due to the serious degradation of PP chains and low branching efficiency of TMPTA.

Comparing with C=C bonds of TMPTA, these of C_{60} are more reactive but not easy to homopolymerize toward free radicals. C_{60} can quickly react with PP macroradicals with the formation of resonance stabilized radicals [Scheme 1, Reaction (1e)], like heteroaromatic ring derivatives.[19,21,22] As shown in Figure 13(b), the β-scission of PP chains was restrained, and more importantly, long chain branched structure was formed during melt radical reaction [Scheme 1, Reaction (1f)]. Therefore, the relaxation time of PP/C_{60} containing DHBP was largely increased.

For PP samples containing TMPTA, C_{60}, and DHBP, most of the PP macroradicals could react with C_{60} to form more stable radicals at first [Scheme 1, Reaction (4f)], and therefore, the homopolymerization of TMPTA was restrained to some extent due to the decreasing content of high reactive radicals. From the above FTIR results, the GD of TMPTA decreased with increasing content of C_{60}, but from the rheological analysis, the contribution of TMPTA in 12T05C010D and 12T12C010D on increasing $G'_{0.01~rad~s^{-1}}$ and $\eta^\star_{0.01~rad~s^{-1}}$ was greater than that in 12T01C010D. As shown in Scheme 1, C_{60} can partially combine with PP macroradicals [Reaction (4f)] and the residual PP macroradicals undergo β-scission reaction [Reaction (4e)] or grafting reaction with TMPTA [Reaction (4g)]. The proportion of Reactions (4e) and (4g) in Sample 12T01C010D was higher than these in Sample 12T05C010D, therefore, as shown in Figure 13(c, d), more TMPTA molecules in Sample 12T01C010D reacted with each other to form homopolymers than these in Samples 12T05C010D or 12T12C010D.

CONCLUSION

Both C_{60} and TMTPA could react with PP macroradicals to prepare HMSPP. However, TMPTA alone underwent homopolymerization to form gel-like particles in the presence of high content of PP macroradicals. Further adding C_{60}, most of the reactive PP macroradicals could be transferred to more stable radicals, and therefore, the homopolymerization of TMPTA was restrained to some extent. From the rheological results, C_{60} and TMPTA showed a synergetic effect on promoting the branching reaction of PP macroradicals and increasing the chain entanglements between PP chains. Considering the functionality of C_{60} in electro-optical properties and improving thermal stabilization for polymers, it is possible to use the resultant HMSPP in the preparation of high-performance nanocomposite foam. However, taking the high price of C_{60} into account, this method has the potential to be further developed by using other reactive nanoparticles in displacement of C_{60}.

ACKNOWLEDGMENTS

REFERENCES

1. Sugimoto, M.; Suzuki, Y.; Hyun, K.; Ahn, K. H.; Ushioda, T.; Nishioka, A.; Taniguchi, T.; Koyama, K. *Rheol. Acta* **2006,** *46*, 33.

2. McCallum, T. J.; Kontopoulou, M.; Park, C. B.; Muliawan, E. B.; Hatzikiriakos, S. G. *Polym. Eng. Sci.* **2007,** *47*, 1133.

3. An, Y. J.; Zhang, Z. J.; Bi, W. G.; Wang, Y. H.; Tang, T. *J. Appl. Polym. Sci.* **2008,** *110*, 3727.

4. Langston, J. A.; Colby, R. H.; Chung, T. C. M.; Shimizu, F.; Suzuki, T.; Aoki, M. *Macromolecules* **2007,** *40*, 2712.

5. Weng, W. Q.; Hu, W. G.; Dekmezian, A. H.; Ruff, C. J. *Macromolecules* **2002,** *35*, 3838.

6. Yoshiga, A.; Otaguro, H.; Parra, D. F.; Lima, L.; Lugao, A. B. *Polym. Bull.* **2009,** *63*, 397.

7. Schulze, D.; Trinkle, S.; Mulhaupt, R.; Friedrich, C. *Rheol. Acta* **2003,** *42*, 251.

8. Tang, H. X.; Dai, W. L.; Chen, B. Q. *Polym. Eng. Sci.* **2008,** *48*, 1339.

9. Cao, K.; Li, Y.; Lu, Z. Q.; Wu, S. L.; Chen, Z. H.; Yao, Z.; Huang, Z. M. *J. Appl. Polym. Sci.* **2011,** *121*, 3384.

10. Li, S. Z.; Xiao, M. M.; Wei, D. F.; Xiao, H. N.; Hu, F. Z.; Zheng, A. N. *Polymer* **2009,** *50*, 6121.

11. Tabatabaei, S. H.; Carreau, P. J.; Ajji, A. *Polym. Eng. Sci.* **2010,** *50*, 191.

12. Tabatabaei, S. H.; Carreau, P. J.; Ajji, A. *Chem. Eng. Sci.* **2009,** *64*, 4719.

13. Cao, X. W.; Zheng, Z. C.; Xie, Y.; Qu, J. P. *Polym. Bull.* **2010,** *64*, 197.

14. Lagendijk, R. P.; Hogt, A. H.; Buijtenhuijs, A.; Gotsis, A. D. *Polymer* **2001,** *42*, 10035.

15. Jorgensen, J. K.; Redford, K.; Ornmundsen, E.; Stori, A. *J. Appl. Polym. Sci.* **2007,** *106*, 950.

16. Graebling, D. *Macromolecules* **2002,** *35*, 4602.

17. Zhang, Z. J.; Xing, H. P.; Qiu, J.; Jiang, Z. W.; Yu, H. O.; Du, X. H.; Wang, Y. H.; Ma, L.; Tang, T. *Polymer* **2010,** *51*, 1593.

18. Zhang, Z. J.; Wan, D.; An, Y. J.; Liu, F.; Xing, H. P.; Wang, L.; Jiang, Z. W.; Tang, T. *Polym. Degrad. Stab.* **2011,** *96*, 653.

19. Wan, D.; Ma, L.; Zhang, Z. J.; Xing, H. P.; Wang, L.; Jiang, Z. W.; Zhang, G. C.; Tang, T. *Polym. Degrad. Stab.* **2012,** *97*, 40.

20. Zhang, Z. J.; Wan, D.; Xing, H. P.; Zhang, Z. J.; Tan, H. Y.; Wang, L.; Zheng, J.; An, Y. J.; Tang, T. *Polymer* **2012,** *53*, 121.

21. Coiai, S.; Passaglia, E.; Aglietto, M.; Ciardelli, F. *Macromolecules* **2004,** *37*, 8414.

22. Coiai, S.; Augier, S.; Pinzino, C.; Passaglia, E. *Polym. Degrad. Stab.* **2010,** *95*, 298.

23. Krusic, P. J.; Wasserman, E.; Keizer, P. N.; Morton, J. R.; Preston, K. F. *Science* **1991,** *254*, 1183.

24. Wan, D.; Zhang, Z. J.; Wang, Y. J.; Xing, H. P.; Jiang, Z. W.; Tang, T. *Soft Matter* **2011,** *7*, 5290.

25. Wan, D.; Wang Y. J.; Wen X.; Qiu J.; Jiang Z. W.; Tan H. Y.; Tang, T. *Polym. Eng. Sci.* **2012, doi: 10.1002/pen.23091.**

26. Guldi, D. M.; Hungerbuhler, H.; Janata, E.; Asmus, K.-D. *J. Chem. Soc. Chem. Commun.* **1993, 84.**

27. Russell, K. E. *Prog. Polym. Sci.* **2002,** *27*, 1007.

28. Romani, F.; Corrieri, R.; Braga, V.; Ciardelli, F. *Polymer* **2002,** *43*, 1115.

29. Zeynalov, E. B.; Allen, N. S.; Salmanova, N. I. *Polym. Degrad. Stab.* **2009,** *94*, 1183.

30. Song, P. A.; Zhu, Y.; Tong, L. F.; Fang Z. P. *Nanotechnology* **2008,** *19*, 225707.

31. Gotsis, A. D.; Zeevenhoven, B. L. F.; Hogt, A. H. *Polym. Eng. Sci.* **2004,** *44*, 973.

32. Münstedt, H.; Schwetz, M.; Heindl, M.; Schmidt, M. *Rheol. Acta* **2001,** *40*, 384.

33. Malmberg, A.; Gabriel, C.; Steffl, T.; Münstedt, H.; Löfgren, B. *Macromolecules* **2001,** *35*, 1038.

34. Malcolm, M. C. *J. Colloid Sci.* **1965,** *20*, 417.

35. Kolodka, E.; Wang, W. J.; Zhu, S. P.; Hamielec, A. E. *Macromolecules* **2002,** *35*, 10062.

36. Vega, J. F.; Santamaria, A.; Munoz-Escalona, A.; Lafuente, P. *Macromolecules* **1998,** *31*, 3639.

37. Van Gurp, M.; Palmen, J. *Rheol. Bull.* **1998,** *67*, 5.

38. Trinkle, S.; Friedrich, C. *Rheol. Acta* **2001,** *40*, 322.

39. Trinkle, S.; Walter, P.; Friedrich, C. *Rheol. Acta* **2002,** *41*, 103.

40. Garcia-Franco, C. A.; Srinivas, S.; Lohse, D. J.; Brant, P. *Macromolecules* **2001,** *34*, 3115.

41. Wang, L.; Wan, D.; Zhang, Z. J.; Liu, F.; Xing, H. P.; Wang, Y. H.; Tang, T. *Macromolecules* **2011,** *44*, 4167.

42. Tian, J. H.; Yu, W.; Zhou, C. X. *Polymer* **2006,** *47*, 7962.